


**Many-Body Critical Phase: Extended and Nonthermal**Yucheng Wang<sup>1,2,3</sup>, Chen Cheng<sup>4</sup>, Xiong-Jun Liu<sup>2,3,5,1,\*</sup> and Dapeng Yu<sup>1</sup><sup>1</sup>*Shenzhen Institute for Quantum Science and Engineering, and Department of Physics, Southern University of Science and Technology, Shenzhen 518055, China*<sup>2</sup>*International Center for Quantum Materials, School of Physics, Peking University, Beijing 100871, China*<sup>3</sup>*Collaborative Innovation Center of Quantum Matter, Beijing 100871, China*<sup>4</sup>*School of Physical Science and Technology, Lanzhou University, Lanzhou 730000, China*<sup>5</sup>*CAS Center for Excellence in Topological Quantum Computation, University of Chinese Academy of Sciences, Beijing 100190, China* (Received 1 November 2019; revised 10 August 2020; accepted 2 February 2021; published 23 February 2021)

The transition between ergodic and many-body localization (MBL) phases lies at the heart of understanding quantum thermalization of many-body systems. Here, we predict a many-body critical (MBC) phase with finite-size scaling analysis in the one-dimensional extended Aubry-André-Harper-Hubbard model, which is different from both the ergodic phase and MBL phase, implying that the quantum system hosts three different fundamental phases in the thermodynamic limit. The level statistics in the MBC phase are well characterized by the so-called critical statistics, and the wave functions exhibit deep multifractal behavior only in the critical region. We further study the half-chain entanglement entropy and thermalization properties and show that the former, in the MBC phase, manifest a volume law scaling, while the many-body states violate the eigenstate thermalization hypothesis. The results are confirmed by the state-of-the-art numerical calculations with system size up to  $L = 22$ . This work unveils a novel many-body phase which is extended but nonthermal.

DOI: [10.1103/PhysRevLett.126.080602](https://doi.org/10.1103/PhysRevLett.126.080602)

*Introduction.*—In the past decade, the eigenstate thermalization hypothesis (ETH) [1–4] has become an essential theoretical underpinning for understanding quantum thermalization physics. Eigenstates in an ergodic phase obey the ETH, while including disorder in interacting systems can lead to the many-body localization (MBL) if the disorder strength is strong enough. The MBL phase violates ETH, i.e., the states in MBL cannot thermalize. The existence of MBL phases has been well established in one-dimensional interacting systems with random disorder [1,5–11] or incommensurate potential [12–24] and has also been observed in interacting ultracold atomic gases trapped in incommensurate optical lattices [25–29].

The nature of the transition from an ergodic phase to MBL remains an active area of research. The entanglement entropy (EE) of eigenstates in an ergodic phase follows the volume law, but in MBL obeys an area law [30–32]. In transition between such two phases, the EE changes in a singular way, rendering an eigenstate phase transition. On the other hand, in view of the long-time dynamics in the ergodic phase and MBL phase [33–38], a dynamical phase transition is manifested between the two phases. The critical features of the transition are also examined in the recent works [21,30,31,39–45] to reveal the nature of the critical points. In particular, an outstanding question is whether there exists some sort of critical phase, other than the critical point in the phase transition. The results based on the finite-size analyses showed that a quantum

critical region in the finite-size interacting system vanishes in the thermodynamic limit [21,43,46–52], for which the emergence of a many-body critical (MBC) phase is yet illusive. To confirm the existence of such a critical phase which is different from both the ergodic and MBL phases is undoubtedly important in understanding the quantum thermalization physics of many body disorder systems.

In this work, we show that a MBC phase can exist in thermodynamic limit in an extended Harper model [53–56] with Hubbard interaction. Employing exact diagonalization (ED) to obtain various diagnostics such as level statistics, multifractality, EE, and thermalization properties, we show, with finite-size scaling analysis, the existence of this new phase of quantum matter which is different from the ergodic and MBL phases and is confirmed with the state-of-the-art numerical study. The level statistics is shown to follow the critical statistics [57–62], and the wave functions exhibit deep multifractal behaviors. Moreover, the eigenstates in this critical phase violate the ETH, but their EE follows a volume law, so this MBC phase is an extended nonthermal phase.

*Model and phase diagram.*—We start with the extended Harper model from the Hamiltonian [53–56]

$$H_0 = \sum_j \left\{ \left( 1 + \mu \cos \left[ 2\pi \left( j + \frac{1}{2} \right) \alpha + \delta \right] \right) c_j^\dagger c_{j+1} + \text{H.c.} \right. \\ \left. + V \cos(2\pi j \alpha + \delta) c_j^\dagger c_j \right\}. \quad (1)$$

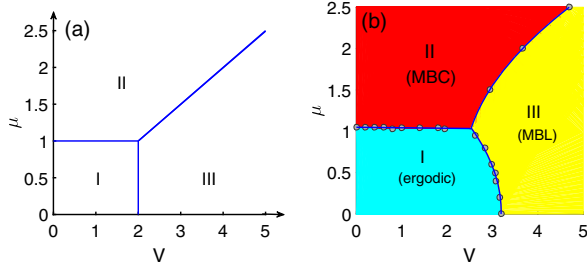


FIG. 1. Main results. (a) Noninteracting phase diagram. The regions I, II, and III correspond to extended, critical, and localized phases, respectively. (b) Phase diagram for the extended interacting Harper model with  $U = 1$ , which contains three phases: the ergodic phase (region I), the MBL phase (region III) and the MBC phase (region II). The transition points (marked by gray dots) can be obtained with finite-size scaling analyses for EE and level statistics, and the phase boundaries are fitted by corresponding curves. Only in the MBC phase of region II, the level statistics follow the critical statistics and the many-body wave functions are multifractal.

where  $c_j$  ( $c_j^\dagger$ ) is the fermion annihilation (creation) operator at the site  $j$ ,  $\mu$  represents the amplitude of the modulation in the off-diagonal hopping,  $V$  is the strength of the on-site incommensurate potential, and  $\delta$  is an arbitrary phase shift. We take  $\alpha = (\sqrt{5} - 1)/2$ , then both the on-site potential and the hopping amplitude between the nearest-neighbor (NN) lattice sites are incommensurate. Figure 1(a) shows the phase diagram of this system [53–56], where the regions I, II, and III correspond to the single-particle extended, critical, and localized phases, respectively. When  $\mu = 0$ , this model is reduced to the Aubry-André-Harper model [63] and  $V = 2$  is the transition point from the extended to the localized phases.

Then, we add the NN repulsive Hubbard interaction and the total Hamiltonian is described by

$$H = H_0 + U \sum_j n_j n_{j+1}, \quad (2)$$

where  $n_j = c_j^\dagger c_j$  is the fermion number operator, and  $U$  represents the interaction strength. We consider the half-filling case, with the numbers of fermions  $N$  and the lattice sites  $L$  being fixed to  $N/L = 1/2$ . Since the sample-to-sample fluctuations in quasiperiodic models are much weaker than those in random disorder models, the number of samples used ranges from 500 to 10 for our study, where a sample is specified by choosing an initial phase  $\delta$ . We obtain the eigenstates by ED under open boundary condition, and, unless otherwise stated, focus on the states in the middle one-third of the spectrum for  $L \leq 18$  and middle 100 states for  $L = 20, 22$  based on the state-of-the-art numerical technique [see, also, Supplemental Material (SM) [64]]. The main results are shown in Fig. 1(b), where the interaction is taken  $U = 1$  as an example. Three fundamental phases, i.e., the ergodic phase (I), the MBL (III), and the MBC phase (II), which constitutes the most important

prediction in this work, are uncovered. Below, we show the phase diagram and further explore the fundamental properties of the MBC phase.

*Energy level statistics and multifractal analysis.*—The MBC phase in region II in Fig. 1(b) can be identified from the energy level statistics and multifractal behavior. We define the energy spacing as  $\delta_n = E_{n+1} - E_n$ , where the eigenvalues  $E_n$  have been listed in ascending order. Then, we can obtain the ratio of adjacent gaps as  $r_n = [\min(\delta_n, \delta_{n+1}) / \max(\delta_n, \delta_{n+1})]$  and average it over all gaps and samples. For the system in the ergodic phase, its level statistics follow Gaussian-orthogonal ensemble (GOE):  $P_G = (\pi/2)(\delta/\langle\delta\rangle)\exp(-\pi\delta^2/4\langle\delta\rangle^2)$ , where  $\langle\delta\rangle$  is the mean spacing and  $\langle r \rangle$  converges to 0.529. In the MBL phase, the level statistics are Poisson:  $P_P = (1/\langle\delta\rangle)\exp(-\delta/\langle\delta\rangle)$  and  $\langle r \rangle \approx 0.387$  [6,7]. The larger  $\langle r \rangle$  in the ergodic phase tells that the spectrum of the ergodic phase is more uniform than that in the MBL phase. However, the value of  $\langle r \rangle$  in region II of Fig. 1(b) is neither 0.387 nor 0.529 (see more details in the SM [64]), implying that the level statistics are neither GOE nor Poisson.

To characterize the statistical properties of the energy spectra in region II, we consider the level number variance  $\Sigma^2(M)$ , which is given by:  $\Sigma^2[M(\epsilon)] = \langle M^2(\epsilon) \rangle - \langle M(\epsilon) \rangle^2$ , with  $\langle M(\epsilon) \rangle$  counting the number of levels in a strip of width  $\epsilon$  on the unfolded scale [47,72,73]. The unfolding procedure is using a smooth function to fit the staircase function  $\eta(E) = \sum_m \Theta(E - E_m)$ , which counts the number of eigenvalues less than and equal to  $E$  (see SM [64]). The angular bracket denotes the average over different regions of the mid-one-third spectrum and different samples. In the MBL phase, the spectrum has no correlations, and therefore, the number variance is exactly linear with slope one, i.e.,  $\Sigma^2(M) = M$  (black solid curve in Fig. 2). The spectrum in the ergodic phase, as mentioned above, is more uniform due to the level repulsion, so the number variance displays a slow logarithmic growth:  $\Sigma^2(M) \approx (2/\pi^2) \ln(2\pi M)$  (red solid curve in Fig. 2) [47,74,75]. The number variance in the MBC phase is qualitatively different, which is linear  $\Sigma^2(M) \sim \chi M$  but with a slope less than one  $\chi < 1$ , as given in Fig. 2. In order to see it clearly, we redisplay the number variance of the critical regime in the inset and confirm that the number variances are asymptotically linear with slopes  $1/2 < \chi < 1$ . The slopes are size insensitive and signify the critical statistics [64,76]. The number variance in the MBC phase is intermediate between the ergodic phase and the MBL phase, which means that the uniformity and the strength of level repulsions of the spectrum are also in between.

We further show the MBC phase through the multifractal analysis based on the system size from 12 to  $L = 22$ , and the analysis can be performed by examining the fractal dimension  $a$  [77,78], defined for each eigenstate  $|n\rangle$  as  $a = -\ln(\sum_j |\psi_j|^4) / \ln D$  with  $D \rightarrow \infty$ , where  $\psi_j$  is the wave function coefficient of the eigenstate  $|n\rangle$  in the

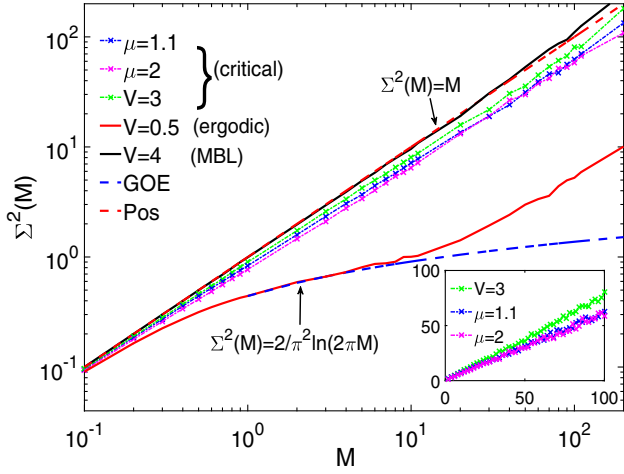


FIG. 2. Number variance  $\Sigma^2(M)$  for different incommensurate potential strengths  $V$  with fixed  $\mu = 0.5$ , and for different  $\mu$  with fixed  $V = 1$ . In the ergodic phase and when  $M$  is small,  $\Sigma^2(M)$  shows a slow logarithmic increase (red solid curve). In the MBL phase,  $\Sigma^2(M)$  is linear with slope one (black solid curve). Inset: Number variance in the critical regime and near the transition point. They are linear with slopes  $1/2 < \chi < 1$ , which is a signature of critical statistics. Here, we fix the number of sites  $L = 16$ .

computational basis  $\{|j\rangle\}$ , given by  $\psi_j = \langle j|n\rangle$ ,  $\langle \sum_j |\psi_j|^4 \rangle$  is the averaged inverse participation ratio (IPR) [79], and  $D = \binom{L}{N}$  is the Hilbert space size. Figure 3(a) shows the fractal dimensions  $a$ , which is obtained by using  $\ln\langle\text{IPR}\rangle = a \ln D + c$  to fit  $\ln\langle\text{IPR}\rangle$  and  $\ln D$  with different sizes, where  $c$  is a constant. We see that  $a \approx 1$  in the ergodic phase, and  $a$  is near 0 (i.e., weak multifractality [52]), which is a consequence of the finite-size effect (see more details in the SM [64]), or  $a = 0$  within error bars (i.e., absence of multifractal behavior) [46,80–82] in the MBL phase. In contrast, the MBC phase is deeply multifractal, with the fractal dimension  $a$  being finite and not close to 0, nor 1, providing a strong evidence for the existence of a new phase different from the ergodic and MBL phases.

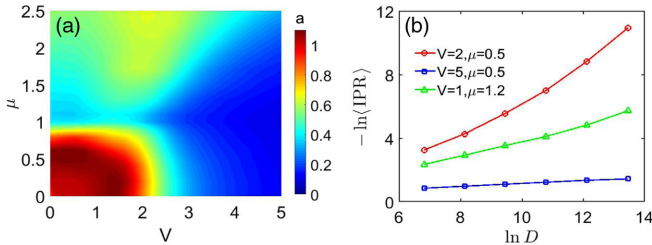


FIG. 3. (a) Fractal dimension  $a$  as a function of  $V$  and  $\mu$ . (b)  $-\ln\langle\text{IPR}\rangle$  as a function of  $\ln D$  with system size varying from  $L = 12$  to  $L = 22$ . The fitting coefficients are  $a = 1.11 \pm 0.15$ ,  $b = -3.48 \pm 1.02$  for  $V = 2$ ,  $\mu = 0.5$  (in the ergodic phase),  $a = 0.0514 \pm 0.0668$ ,  $b = 0.21 \pm 0.04$  for  $\mu = 0.5$ ,  $V = 5$  (in the MBL phase, the range of  $a$  covers 0) and  $a = 0.51 \pm 0.08$ ,  $b = -0.77 \pm 0.28$  for  $V = 1$ ,  $\mu = 1.2$  (in the MBC phase).

Further, more careful analysis shows a logarithmic sub-leading correction to the scaling of  $\langle\text{IPR}\rangle$ , i.e.,  $-\ln\langle\text{IPR}\rangle = a \ln D + b \ln(\ln D) + o(\ln D)$ . We find that  $b$  is negative, negative, and positive for the ergodic, MBC, and MBL phases, respectively [Fig. 3(b)], as summarized in Table I.

The critical level statistics and deep multifractal behavior of many-body wave functions show that region II in Fig. 1(b) is a MBC phase, qualitatively different from both the ergodic and MBL phases. An intuitive understanding for the existence of the MBC phase with interactions is given in the SM by connecting the many-body wave function and single-particle orbits [64]. Next, we proceed to study the EE and thermalization with finite-size scaling analyses, which confirm the critical points of phase transition in the thermodynamic limit and give characteristic features of the MBC phase.

*Finite-size scaling and entanglement entropy.*—The EE is an important resource for exploring the critical behaviors and the localization features of many-body states based on finite-size scaling analysis. For a correlated system, the EE is obtained by  $S = -\sum_i \lambda_i \ln \lambda_i$ , where  $\lambda_i$  is the  $i$ th eigenvalue of a reduced density matrix, which can be obtained by tracing out half of this system. We find that different energy windows have little effect on the EE in the ergodic and MBL phases (see more details in the SM [64]), so we can consider the average EE  $\langle S \rangle$  averaged over the mid-one-third states for  $L = 16, 18$  and over the mid-100 states for  $L = 20, 22$ , as showed in Fig. 4. From Fig. 4(a), one can see that the average EE follows a volume law in the ergodic phase while it decreases to a constant independent of  $L$  in the deep MBL phase, which fulfills an area law. Unlike the MBL, we show, in Fig. 4(b), that the average EE follows a volume law when the system is the critical phase. The EE in the ergodic phase gives the maximum EE well, i.e.,  $\langle S \rangle = \ln \Omega = \ln 2^{L/2} = \frac{L}{2} \ln 2$ , where  $\Omega$  is the total number of states of the half-chain. The average EE in the MBC phase, however, is clearly less than the maximum EE, so the MBC phase is extended but nonergodic. For a more precise study, we perform a finite-size scaling analysis for the EE which is rescaled by the page value  $S_T = 0.5[L \ln 2 - 1]$  [83,84], as shown in Figs. 4(c) and 4(d), where the results are fit to  $\langle S/S_T \rangle = f[(V - V_c)L^{1/\nu}]$  with fixed  $\mu = 0.5$ , and  $\langle S/S_T \rangle = g[(\mu - \mu_c)L^{1/\nu}]$  with fixed  $V = 1$ , respectively. Here,  $V_c$  and  $\mu_c$  denote the transition point from the ergodic phase to the MBL and MBC phases, respectively, and  $\nu$  is the associated critical exponent. In

TABLE I. A comparison of the coefficients  $a$  and  $b$  in different phases.

Coefficients	Phases
$a \approx 1, b < 0$	Ergodic phase
$a$ is far from 0 and 1, $b < 0$	MBC phase
$a$ is near 0 or $a = 0, b > 0$	MBL phase

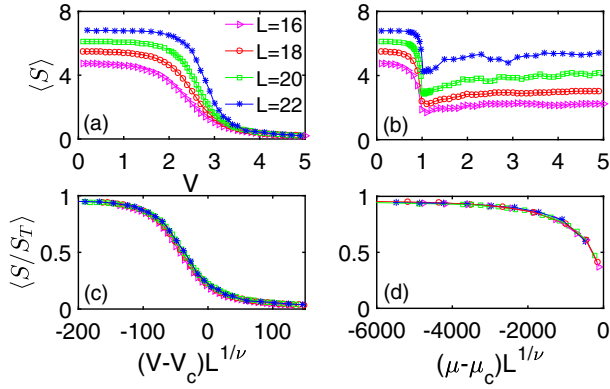


FIG. 4. (a) The sample averaged EE  $\langle S \rangle$  as a function of  $V$  with fixed  $\mu = 0.5$  and (b)  $\langle S \rangle$  as a function of  $\mu$  with fixed  $V = 1$ . Finite-size scaling analysis of  $\langle S/S_T \rangle$  as a function of  $(V - V_c)L^{1/\nu}$  with fixed  $\mu = 0.5$  in (c) and  $(\mu - \mu_c)L^{1/\nu}$  with fixed  $V = 1$  in (d). Rescaled  $\langle S/S_T \rangle$  so that all curves for different sizes converge to a single curve. Here, the number of the samples is (50,10,100,50) for  $L = (16, 18, 20, 22)$ .

confirming the existence of phase transition, it is sufficient to perform the finite-size analysis only in one side of the critical points, say with  $\mu < \mu_c$ . The results of the best fit are (c)  $V_c = 3.08 \pm 0.05$  and  $\nu = 0.71 \pm 0.06$  and (d)  $\mu_c = 1.03 \pm 0.05$  and  $\nu = 0.32 \pm 0.03$ , which are doubly confirmed with the same results obtained by performing the finite-size scaling analyses for energy level statistics [64]. The critical exponent  $\nu$  can be determined similarly for generic parameters  $V$  and  $\mu$  near the phase boundaries, and exhibits a variation range in the whole phase boundaries with different  $V_c$  and  $\mu_c$ , which is typical for disordered systems. The approximate ranges are

$$\nu = \begin{cases} 0.6(0) \sim 0.8(2), & \text{for I} \rightarrow \text{III}, \\ 0.3(5) \sim 0.4(7), & \text{for I} \rightarrow \text{II}, \\ 0.6(5) \sim 0.8(4), & \text{for II} \rightarrow \text{III}, \end{cases} \quad (3)$$

where I, II, and III are the ergodic, MBC, and MBL phases, respectively.

Note that a finite-size system may exhibit a critical region near the transition point between the ergodic and MBL phases [39–43] when the system size is smaller than the correlation length (for the ergodic phase) or localization length (for the MBL phase). The critical region vanishes in the thermodynamic limit after performing finite-size analyses [43]. In contrast, from the finite-size scaling analysis, we confirm that the MBC phase predicted here exists in the thermodynamic limit.

*Thermalization properties.*—Finally, we study the thermalization properties of the MBC phase. For this, we consider the average deviation of the half-chain particle-number distribution from the half-number ( $N/2$ ) of particles, which can characterize the thermalization of the system and

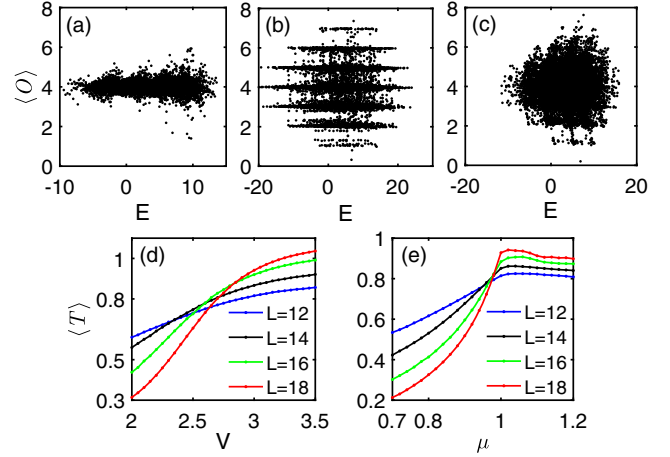


FIG. 5. The observable  $O(E)$  versus eigenvalues for (a)  $V = 1$ ,  $\mu = 0.5$  in the ergodic phase, (b)  $V = 4$ ,  $\mu = 0.5$  in the MBL phase and (c)  $V = 1$ ,  $\mu = 1.2$  in the MBC phase. Here, the system size has been fixed as  $L = 2N = 16$  and the initial phase  $\delta = 0$ .  $\langle T \rangle$  as a function of (d)  $V$  with fixed  $\mu = 0.5$  and (e)  $\mu$  with fixed  $V = 1$  for different sizes.

is defined by  $T = \{ [1/(D_2 - D_1)] \sum_{m=D_1}^{D_2} [O(E_m) - N/2]^2 \}^{1/2}$ , with many-body eigenstates of eigenvalue  $E_m$  being summed over. Here, the observable  $O(E) = \sum_{j=1}^{L/2} \langle \psi_E | n_j | \psi_E \rangle$  quantifies the number of particles distributed in the half chain of the lattice for the many-body eigenstate  $|\psi_E\rangle$  with energy  $E$  [14]. The large fluctuation of  $O(E)$  among nearby eigenstates signifies the violation of the ETH. In the ergodic phase, the fluctuations of  $O$  are small and the ETH is satisfied [Fig. 5(a)], while in the MBL phase, the fluctuations are obviously larger and the ETH is violated [Fig. 5(b)]. For parameters in the critical regime, as shown in Fig. 5(c), the fluctuations of  $O$  are also large, which implies that the ETH is violated and the eigenstates are nonthermal. This feature can be even clearer by examining the qualitative behaviors of  $T$  defined for the mid-one-third of states with  $D_1 = D/3$  and  $D_2 = 2D/3$ . As the system size  $L$  increases, the value  $O(E)$  tends to  $N/2$  in the ergodic phase but keeps fluctuating and results in finite values of  $T$  at large  $L$  for the nonthermal phase. The numerical results of the sample averaged  $\langle T \rangle$  are presented in Figs. 5(d) and 5(e), as a function of  $V$  and  $\mu$ . With the increasing of system size  $L$ , we see that  $\langle T \rangle$  decreases if the phase is ergodic but enlarges in the MBL and MBC phases. Therefore, the critical phase is nonthermal, similar to the MBL phase. Together with the preceding discussion on the EE, we conclude that the MBC phase is an extended nonthermal phase.

*Conclusions.*—We have predicted that a MBC phase exists in the thermodynamic limit in the 1D extended Aubry-André-Harper-Hubbard model. Being a third type of fundamental phase, distinct from ergodic and MBL phases, the MBC phase shows novel basic features. First, by analyzing number variance, we found that the level statistics in the critical phase are neither GOE for ergodic

regime nor Poisson for MBL, but are well described by critical statistics. Further, from a multifractal analysis, we showed that the many-body states in the MBC phase exhibit the deep multifractal behavior. Finally, we unveiled that the predicted critical phase violates the ETH, but the EE exhibits a volume law, implying that this exotic critical phase is delocalized but nonergodic and not thermal. Our conclusive results are confirmed with system size up to  $L = 22$  by the state-of-the-art numerical method. As a new interacting phase beyond the ergodic and MBL phases, many interesting issues, including the dynamical properties, deserve further efforts of study. Our work opens a door to explore quantum thermalization physics in the MBC phases.

We thank Xiaopeng Li for valuable discussions. This work was supported by National Nature Science Foundation of China (Grants No. 11761161003, No. 11825401, and No. 11921005), the National Key R&D Program of China (Grant No. 2016YFA0301604), Guangdong Innovative and Entrepreneurial Research Team Program (Grant No. 2016ZT06D348), the Science, Technology, and Innovation Commission of Shenzhen Municipality (Grant No. KYTDPT20181011104202253), the Open Project of Shenzhen Institute of Quantum Science and Engineering (Grant No. SIQSE202003), and the Strategic Priority Research Program of the Chinese Academy of Science (Grant No. XDB28000000). C.C. is supported by the National Natural Science Foundation of China (Grant No. 11904145). The computations were partially performed in the Tianhe-2JK at the Beijing Computational Science Research Center.

\*Corresponding author.

xionjunliu@pku.edu.cn

- [1] R. Nandkishore and D. A. Huse, *Annu. Rev. Condens. Matter Phys.* **6**, 15 (2015).
- [2] J. M. Deutsch, *Phys. Rev. A* **43**, 2046 (1991).
- [3] M. Rigol, V. Dunjko, and M. Olshanii, *Nature (London)* **452**, 854 (2008).
- [4] J. M. Deutsch, *Rep. Prog. Phys.* **81**, 082001 (2018).
- [5] D. M. Basko, I. L. Aleiner, and B. L. Altshuler, *Ann. Phys. (Amsterdam)* **321**, 1126 (2006).
- [6] V. Oganesyan and D. A. Huse, *Phys. Rev. B* **75**, 155111 (2007).
- [7] A. Pal and D. A. Huse, *Phys. Rev. B* **82**, 174411 (2010).
- [8] E. Altman and R. Vosk, *Annu. Rev. Condens. Matter Phys.* **6**, 383 (2015).
- [9] R. Vosk, D. A. Huse, and E. Altman, *Phys. Rev. X* **5**, 031032 (2015).
- [10] M. Žnidarič, A. Scardicchio, and V. K. Varma, *Phys. Rev. Lett.* **117**, 040601 (2016).
- [11] L. Faoro, M. V. Feigel'man, and L. Ioffe, *Ann. Phys. (Amsterdam)* **409**, 167916 (2019).
- [12] S. Iyer, V. Oganesyan, G. Refael, and D. A. Huse, *Phys. Rev. B* **87**, 134202 (2013).
- [13] R. Modak and S. Mukerjee, *Phys. Rev. Lett.* **115**, 230401 (2015).
- [14] X. Li, S. Ganeshan, J. H. Pixley, and S. Das Sarma, *Phys. Rev. Lett.* **115**, 186601 (2015).
- [15] X. Li, J. H. Pixley, D.-L. Deng, S. Ganeshan, and S. Das Sarma, *Phys. Rev. B* **93**, 184204 (2016).
- [16] Y. Wang, H. Hu, and S. Chen, *Eur. Phys. J. B* **89**, 77 (2016).
- [17] M. Lee, T. R. Look, S. P. Lim, and D. N. Sheng, *Phys. Rev. B* **96**, 075146 (2017).
- [18] A. Chandran and C. R. Laumann, *Phys. Rev. X* **7**, 031061 (2017).
- [19] S. Nag and A. Garg, *Phys. Rev. B* **96**, 060203(R) (2017).
- [20] J. Gray, S. Bose, and A. Bayat, *Phys. Rev. B* **97**, 201105(R) (2018).
- [21] F. Setiawan, D.-L. Deng, and J. H. Pixley, *Phys. Rev. B* **96**, 104205 (2017).
- [22] P. J. D. Crowley, A. Chandran, and C. R. Laumann, *Phys. Rev. Lett.* **120**, 175702 (2018).
- [23] S.-X. Zhang and H. Yao, *Phys. Rev. Lett.* **121**, 206601 (2018).
- [24] E. V. H. Doggen and A. D. Mirlin, *Phys. Rev. B* **100**, 104203 (2019).
- [25] M. Schreiber, S. S. Hodgman, P. Bordia, H. P. Lüschen, M. H. Fischer, R. Vosk, E. Altman, U. Schneider, and I. Bloch, *Science* **349**, 842 (2015).
- [26] P. Bordia, H. P. Lüschen, S. S. Hodgman, M. Schreiber, I. Bloch, and U. Schneider, *Phys. Rev. Lett.* **116**, 140401 (2016).
- [27] P. Bordia, H. Lüschen, S. Scherg, S. Gopalakrishnan, M. Knap, U. Schneider, and I. Bloch, *Phys. Rev. X* **7**, 041047 (2017).
- [28] H. P. Lüschen, P. Bordia, S. Scherg, F. Alet, E. Altman, U. Schneider, and I. Bloch, *Phys. Rev. Lett.* **119**, 260401 (2017).
- [29] T. Kohlert, S. Scherg, X. Li, H. P. Lüschen, S. Das Sarma, I. Bloch, and M. Aidelsburger, *Phys. Rev. Lett.* **122**, 170403 (2019).
- [30] J. A. Kjäll, J. H. Bardarson, and F. Pollmann, *Phys. Rev. Lett.* **113**, 107204 (2014).
- [31] T. Grover, arXiv:1405.1471.
- [32] B. Bauer and C. Nayak, *J. Stat. Mech.* (2013) P09005.
- [33] R. Vosk and E. Altman, *Phys. Rev. Lett.* **110**, 067204 (2013).
- [34] M. Serbyn and Z. Papić, and D. A. Abanin, *Phys. Rev. Lett.* **111**, 127201 (2013).
- [35] M. Serbyn, M. Knap, S. Gopalakrishnan, Z. Papić, N. Y. Yao, C. R. Laumann, D. A. Abanin, M. D. Lukin, and E. A. Demler, *Phys. Rev. Lett.* **113**, 147204 (2014).
- [36] M. Žnidarič, T. Prosen, and P. Prelovšek, *Phys. Rev. B* **77**, 064426 (2008).
- [37] J. H. Bardarson, F. Pollmann, and J. E. Moore, *Phys. Rev. Lett.* **109**, 017202 (2012).
- [38] E. J. Torres-Herrera and L. F. Santos, *Phys. Rev. B* **92**, 014208 (2015).
- [39] K. Agarwal, S. Gopalakrishnan, M. Knap, M. Müller, and E. Demler, *Phys. Rev. Lett.* **114**, 160401 (2015).
- [40] D. Pekker, G. Refael, E. Altman, E. Demler, and V. Oganesyan, *Phys. Rev. X* **4**, 011052 (2014).
- [41] R. Vasseur, A. C. Potter, and S. A. Parameswaran, *Phys. Rev. Lett.* **114**, 217201 (2015).

- [42] E. J. Torres-Herrera and L. F. Santos, *Ann. Phys. (Amsterdam)* **529**, 1600284 (2017).
- [43] V. Khemani, S. P. Lim, D. N. Sheng, and D. A. Huse, *Phys. Rev. X* **7**, 021013 (2017).
- [44] M. Pino, V. E. Kravtsov, B. L. Altshuler, and L. B. Ioffe, *Phys. Rev. B* **96**, 214205 (2017).
- [45] M. Rispoli, A. Lukin, R. Schittko, S. Kim, M. E. Tai, J. Léonard, and M. Greiner, *Nature (London)* **573**, 385 (2019).
- [46] D. J. Luitz, N. Laflorencie, and F. Alet, *Phys. Rev. B* **91**, 081103(R) (2015).
- [47] C. L. Bertrand and A. M. García-García, *Phys. Rev. B* **94**, 144201 (2016).
- [48] K. Kudo and T. Deguchi, *Phys. Rev. B* **97**, 220201(R) (2018).
- [49] A. C. Potter, R. Vasseur, and S. A. Parameswaran, *Phys. Rev. X* **5**, 031033 (2015).
- [50] S. Parameswaran, A. C. Potter, and R. Vasseur, *Ann. Phys. (Amsterdam)* **529**, 1600302 (2017).
- [51] P. T. Dumitrescu, A. Goremykina, S. A. Parameswaran, M. Serbyn, and R. Vasseur, *Phys. Rev. B* **99**, 094205 (2019).
- [52] N. Macé, F. Alet, and N. Laflorencie, *Phys. Rev. Lett.* **123**, 180601 (2019).
- [53] Y. Hatsugai and M. Kohmoto, *Phys. Rev. B* **42**, 8282 (1990).
- [54] J. H. Han, D. J. Thouless, H. Hiramoto, and M. Kohmoto, *Phys. Rev. B* **50**, 11365 (1994).
- [55] Y. Takada, K. Ino, and M. Yamanaka, *Phys. Rev. E* **70**, 066203 (2004).
- [56] F. Liu, S. Ghosh, and Y. D. Chong, *Phys. Rev. B* **91**, 014108 (2015).
- [57] B. I. Shklovskii, B. Shapiro, B. R. Sears, P. Lambrianides, and H. B. Shore, *Phys. Rev. B* **47**, 11487 (1993).
- [58] K. A. Muttalib, Y. Chen, M. E. H. Ismail, and V. N. Nicopoulos, *Phys. Rev. Lett.* **71**, 471 (1993).
- [59] M. Moshe, H. Neuberger, and B. Shapiro, *Phys. Rev. Lett.* **73**, 1497 (1994).
- [60] V. E. Kravtsov and K. A. Muttalib, *Phys. Rev. Lett.* **79**, 1913 (1997).
- [61] S. M. Nishigaki, *Phys. Rev. E* **59**, 2853 (1999).
- [62] A. M. García-García and J. J. M. Verbaarschot, *Phys. Rev. E* **67**, 046104 (2003).
- [63] S. Aubry and G. André, *Ann. Isr. Phys. Soc.* **3**, 133 (1980).
- [64] See Supplemental Material at <http://link.aps.org/supplemental/10.1103/PhysRevLett.126.080602> for details on (I) finite size scaling for energy level statistics; (II) unfolding procedure; (III) scaling analysis; and (IV) characterizing different phases from one-particle perspective, which includes Refs. [33,34,47,48,65–71].
- [65] M. Serbyn and J. E. Moore, *Phys. Rev. B* **93**, 041424(R) (2016).
- [66] F. Pietracaprina, N. Macé, D. J. Luitz, and F. Alet, *SciPost Phys.* **5**, 045 (2018).
- [67] M. S. S. Challa and D. P. Landau, *Phys. Rev. B* **33**, 437 (1986).
- [68] S. V. Isakov and R. Moessner, *Phys. Rev. B* **68**, 104409 (2003).
- [69] Y. Wang, Y. Wang, and S. Chen, *Eur. Phys. J. B* **89**, 254 (2016).
- [70] S. Bera, H. Schomerus, F. Heidrich-Meisner, and J. H. Bardarson, *Phys. Rev. Lett.* **115**, 046603 (2015).
- [71] S. Bera, T. Martyneć, H. Schomerus, F. Heidrich-Meisner, and J. H. Bardarson, *Ann. Phys. (Amsterdam)* **529**, 1600356 (2017).
- [72] F. J. Dyson and M. L. Mehta, *J. Math. Phys. (N.Y.)* **4**, 701 (1963).
- [73] T. Guhr, A. Müller-Groeling, and H. A. Weidenmüller, *Phys. Rep.* **299**, 189 (1998).
- [74] When  $M$  is bigger, the number variance in the ergodic phase shows a much faster power-law growth, which is considered to be an evidence of the existence of the Thouless energy [75].
- [75] D. Braun and G. Montambaux, *Phys. Rev. B* **52**, 13903 (1995).
- [76] The critical statistics can be used to describe the energy spectrum of a high-dimensional, noninteracting disordered system near the extended-Anderson localization transition point.
- [77] R. J. Bell, *Rep. Prog. Phys.* **35**, 1315 (1972).
- [78] D. J. Luitz, F. Alet, and N. Laflorencie, *Phys. Rev. Lett.* **112**, 057203 (2014).
- [79] D. J. Thouless, *Phys. Rep.* **13**, 93 (1974).
- [80] D. J. Luitz and Y. B. Lev, *Ann. Phys. (Berlin)* **529**, 1600350 (2017).
- [81] X. Wei, R. Mondaini, and X. Gao, [arXiv:2001.04105](https://arxiv.org/abs/2001.04105).
- [82] We note that the numerical data in Ref. [52] essentially shows the nontrivial multifractality around the critical transition point of a many-body localization, and for the deep MBL phase far away from the critical point, the multifractality is negligibly small. This is well consistent with our current interpretation that the multifractality exists for the critical phase. For a system with finite size, there exists a critical region [39–43,64] near the transition point between MBL and the ergodic phase, and the nonzero fractal dimension  $a$  in the MBL phase near the transition point essentially reflects the multifractal behaviors in the critical regime. In the thermodynamic limit, the nonzero fractal dimension should be obtained only precisely at the critical point, not in the MBL phase.
- [83] V. Khemani, D. N. Sheng, and D. A. Huse, *Phys. Rev. Lett.* **119**, 075702 (2017).
- [84] D. N. Page, *Phys. Rev. Lett.* **71**, 1291 (1993).